JOURNAL OF Applied Polymer SCIENCE

Joint flame-retardant effect of triazine-rich and triazine/phosphaphenanthrene compounds on epoxy resin thermoset

Yong Qiu, Lijun Qian, Wang Xi, Xinxin Liu
Department of Materials Science and Engineering, Beijing Technology and Business University, Beijing 100048, People's Republic of China
Correspondence to: L. Qian (E-mail: qianlj@th.btbu.edu.cn)

ABSTRACT: To obtain a more efficient flame-retardant system, the extra-triazine-rich compound melamine cyanurate (MCA) was coworked with tri(3-9,10-dihydro-9-oxa-10-phosphaphenanthrene-10-oxide-2-hydroxypropan-1-yl)−1,3,5-triazine-2,4,6-trione (TGIC–DOPO) in epoxy thermosets; these were composed of diglycidyl ether of bisphenol A (DGEBA) epoxy resin and 4,4′-diaminodiphenyl methane (DDM). The flame-retardant properties were investigated by limited oxygen index measurement, vertical burning testing, and cone calorimeter testing. In contrast to the DGEBA/DDM (EP for short) thermoset with a single TGIC–DOPO, a better flame retardancy was obtained with TGIC–DOPO/MCA/EP. The 3% TGIC–DOPO/2% MCA/EP thermoset showed a lower peak heat-release rate value, a lower effective heat of combustion value, fewer total smoke products, and lower total yields of carbon monoxide and carbon dioxide in comparison with 3% TGIC–DOPO/EP. The results reveal that MCA and TGIC–DOPO worked jointly in flame-retardant thermosets. The dilution effect of MCA, the quenching effect of TGIC–DOPO, and their joint action inhibited the combustion intensity and imposed a better flame-retardant effect in the gas phase. The 3% TGIC–DOPO/2% MCA/EP thermoset also exhibited an increased residue yield, and more compositions with triazine rings were locked in the residues; this implied that MCA/TGIC–DOPO worked jointly in the condensed phase and promoted thermoset charring. The results reveal the better flame-retardant effect of the MCA/TGIC–DOPO system in the condensed phase. Therefore, the joint incorporation of MCA and TGIC–DOPO into the EP thermosets increased the flame-retardant effects in both the condensed and gas phases during combustion. This implied that the adjustment to the group ratio in the flame-retardant group system endowed the EP thermoset with better flame retardancy. © 2015 Wiley Periodicals, Inc. J. Appl. Polym. Sci. **2016**, *133*, 43241.

KEYWORDS: composites; flame retardance; thermosets

Received 31 July 2015; accepted 19 November 2015
DOI: 10.1002/app.43241

INTRODUCTION

Flame-retardant modification is an effective way to impose flame retardancy to flammable materials.[1–3] To construct novel flame retardants with higher flame-retardant efficiencies, many researches have combined some known efficient characteristic structures or functional groups together; these have included triazine,[4] cyclotriphosphazene,[5] phosphaphenanthrene,[6] silsesquioxane,[7] and phosphonate.[8] This has become one of the most feasible methods for obtaining more economic and efficient flame retardants or flame-retardant systems.[9–12] Moreover, the combining methods can be divided into chemical combination and physical compounding. Silsesquioxane-graphene compound,[13] silane-(spirocyclic pentaerythritol bisphosphorate)-phosphaphenanthrene compound,[14] and fullerene-(bicyclicpentaerythritol phosphate) compound[15] have been constructed by chemical combination to separately enhance the flame retardancy of polycarbonate and ethylene vinyl acetate copolymers. Meanwhile, by physical compounding, aluminum hypophosphite/melamine cyanurate (MCA),[16] aluminum diethyl phosphinate/MCA,[17] aluminum dipropyl phosphinate/melamine,[18] and ammonium polyphosphate (APP)/melamine polyphosphate/titanium dioxide[19] composites have been applied to the preparation of flame-retardant poly(ethylene terephthalate), poly(1,4-butylene terephthalate), polyamide 6, and poly(methyl methacrylate), respectively. APP/ethylenediamine-(*N*,*N*-diphenyl triazine),[20] APP/hyperbranched ethane diamine–triazine,[21] and melamine pyrophosphate/diethylenetriamine–(ethanolamine–triazine)[22] composites have been used to improve the flame retardancy of polypropylene. Similarly, APP/hyperbranched (aromatic diamine)–triazine[23] composites have also imposed excellent flame retardancy to acrylonitrile–butadiene–styrene resin.

As the fundamental materials in the electrical and electronics industries, epoxy resins need to have their flame retardancy improved either by chemical combination or physical compounding modification.[24–27] Several highly efficient flame retardants with bigroup or multigroup compounds have been designed and synthesized by chemical combination; examples include

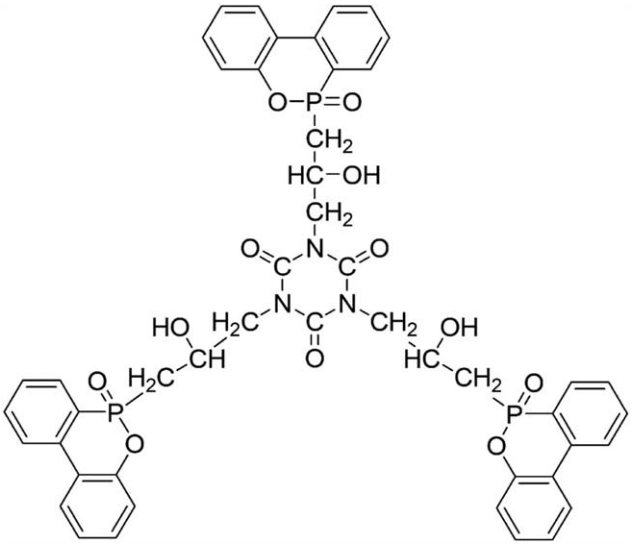

Scheme 1. The chemical structure of TGIC-DOPO

(phosphazene-phosphaphenanthrene compound,[28,29] triazene-phosphaphenanthrene compound),[30] phosphaphenanthrene-(triazine-trione) compound,[31,32] and phosphaphenanthrene-ester-(triazine-trione) compound.[33–35] Simultaneously, APP/MCA[36,37] and octaphenyl polyhedral oligomeric silsesquioxane/9,10-dihydro-9-oxa-10-phosphaphenanthrene-10-oxide composites[38] have also been applied in epoxy resin thermosets for better flame retardancy through physical compounding.

Similarly, in our previous research work,[39] a novel bigroup flame retardant, tri(3-9,10-dihydro-9-oxa-10-phosphaphenanthrene-10-oxide-2-hydroxypropan-1-yl)−1,3,5-triazine-2,4,6-trione (TGIC–DOPO; Scheme 1) was designed and synthesized successfully. This compound presented a desirable efficiency in a flame-retardant epoxy resin thermoset. Moreover, the high-efficiency flame-retardant mechanism of TGIC–DOPO in the condensed and gas phases was also revealed and was ascribed to the synergistic effect between the phosphaphenanthrene and triazine groups. Hence, the following questions were put forward. Did the phosphaphenanthrene/triazine group ratio affect the flame-retardant effect of TGIC–DOPO on the epoxy resin thermoset? Did the specific phosphaphenanthrene/triazine group ratio endow the system with a higher flame-retardant efficiency?

To verify the aforementioned conjectures, the triazine-rich flame retardant MCA was adopted to work jointly with TGIC–DOPO in diglycidyl ether of bisphenol A epoxy resin cured with 4,4′-diaminodiphenyl methane (EP for short). The research results demonstrate the joint flame-retardant effect on EP thermosets. Thus, the flame-retardant behaviors of TGIC–DOPO/MCA/EP were researched, and the flame-retardant mechanism of TGIC–DOPO/MCA was also explored.

EXPERIMENTAL

Materials

Diglycidyl ether of bisphenol A (DGEBA; E-51, purity ≥ 99.0%) was supplied by Blue Star New Chemical Material Co., Ltd. (China). 4,4′-Diaminodiphenyl methane (DDM; purity ≥ 99.0%) was purchased from Sinopharm Chemical Reagent Co., Ltd. (China). TGIC–DOPO (purity = 93.6%, the impurities consisted of oligomeric byproducts) was synthesized in our laboratory.[39] MCA (Melapur MC 25, purity = 99.2%) was produced by BASF-Ciba.

Preparation of the TGIC–DOPO/MCA/EP Thermosets

TGIC–DOPO and MCA were added to the DGEBA epoxy resin with mechanical stirring at room temperature. The mixture was then heated slowly to 130°C and stirred until TGIC–DOPO melted and completely dissolved in DGEBA. Subsequently, the TGIC–DOPO/MCA/DGEBA mixture was cooled to 100°C. The curing agent (DDM) was then added to the mixture and mixed adequately to form a uniform mixed system. After 3 min of degassing in a vacuum oven at 100°C, the prepared resin was poured into preheated molds and cured at 120°C for 2 h and then at 170°C for 4 h.[40]

Preparation of the Control Sample Thermosets

TGIC–DOPO/EP. The TGIC–DOPO/EP thermosets were prepared with the same method that was used to prepare the TGIC–DOPO/MCA/EP thermosets but without the addition of MCA.

MCA/EP. MCA was added to the epoxy resin DGEBA with mechanical stirring at room temperature. The mixture was then heated slowly to 100°C. Subsequently, DDM was added to the mixture and mixed adequately to form a uniform mixed system. After it was degassed for 3 min in a vacuum oven at 100°C, the prepared resin was poured into preheated

Table I. Formulations of the Epoxy Resin Thermosets

			TGIC–DOPO		MCA	
Sample	DGEBA (g)	DDM (g)	g	wt %	g	wt %
EP	100	25.3	—	—	—	—
1% TGIC–DOPO/2% MCA/EP	100	25.3	1.29	1.0%	2.58	2.0%
2% TGIC–DOPO/2% MCA/EP	100	25.3	2.61	2.0%	2.61	2.0%
3% TGIC–DOPO/2% MCA/EP	100	25.3	3.96	3.0%	2.64	2.0%
1% TGIC–DOPO/EP	100	25.3	1.27	1.0%	—	—
2% TGIC–DOPO/EP	100	25.3	2.56	2.0%	—	—
3% TGIC–DOPO/EP	100	25.3	3.88	3.0%	—	—
2% MCA/EP	100	25.3	—	—	2.56	2.0%

Table II. LOI and UL94 Data for the Epoxy Resin Thermosets

		Vertical burning test			
		After-flame time			
Sample	LOI (%)	$\bar{t}_1$(s)	$\bar{t}_2$(s)	UL94 rating	Dripping
EP	26.4	83.0[a]	—	Unrated	Yes
1% TGIC-DOPO/2% MCA/EP	31.1	22.8	10.2	Unrated	No
2% TGIC-DOPO/2% MCA/EP	33.1	7.2	4.4	V-1	No
3% TGIC-DOPO/2% MCA/EP	34.0	1.5	3.6	V-0	No
1% TGIC-DOPO/EP	31.3	15.4	21.6	Unrated	No
2% TGIC-DOPO/EP	32.5	8.2	4.7	V-1	No
3% TGIC-DOPO/EP	34.9	4.3	8.2	V-1	No
2%MCA/EP	27.3	45.8[a]	—	Unrated	No

[a] The after flame of the specimen burned to the clamp in the first flame application.
[b] $\bar{t}_1$ and $\bar{t}_2$ are the after-flame time of the first and second flame application, respectively.

molds and cured at 120°C for 2 h and then at 170°C for 4 h.[40]

DGEBA/DDM (EP). The EP thermoset was also prepared with the same method that was used to prepare the MCA/EP thermoset but without the addition of MCA.

The formulations of the developed systems are listed in Table I.

Characterization

The limited oxygen index (LOI) value was measured with an oxygen index instrument produced by Fire Testing Technology, Ltd. (United Kingdom, sample dimensions: 130 × 6.5 × 3.2 mm^3, ASTM D 2863-13). The UL94 flame-retardant rating was obtained with a horizontal/vertical flame chamber produced by Fire Testing Technology, Ltd. (sample dimensions: 125 × 12.7 × 3.2 mm^3, ASTM D 3801-10). Cone calorimetry testing was conducted at an external heat flux of 50 kW/m^2 with a cone calorimeter produced by Fire Testing Technology, Ltd. (sample dimensions: 100 × 100 × 3 mm^3, ISO 5660-1). The cone calorimetry test for each sample was conducted three times.

The Fourier transform infrared (FTIR) spectra were obtained with a Nicolet iN10MX-type spectrometer. The limited oxygen index residue crown (LOI-RC) and limited oxygen index residue mandril (LOI-RM) samples were selected from specimens that self-extinguished within 1 to 2 min and had an extent of burning of less than 50 mm from the top. The residue samples were thoroughly mixed with KBr and pressed into pellets.

The pyrolytic fragments were recognized by a Shimadzu GC-MS-QP5050A gas chromatography/mass spectrometry apparatus equipped with a PYR-4A pyrolyzer. Helium (He) was used as a carrier gas for the volatile products. The injector temperature was 250°C, the temperature of the gas chromatography/mass spectrometry interface was 280°C, and the cracker temperature was 500°C.

The elemental compositions of LOI-RC and LOI-RM were investigated with a PerkinElmer PHI 5300 ESCA X-ray photoelectron spectrometer. The residues were selected from specimens that self-extinguished within 1 to 2 min and had an extent of burning of less than 50 mm from the top; they were sufficiently ground and mixed before analysis. The X-ray photoelectron spectrometry tests for each specimen were conducted three times.

RESULTS AND DISCUSSION

LOI Measurement and Vertical Burning Testing

Generally, the flame retardancy of materials can be measured easily via LOI measurement and vertical burning testing, which

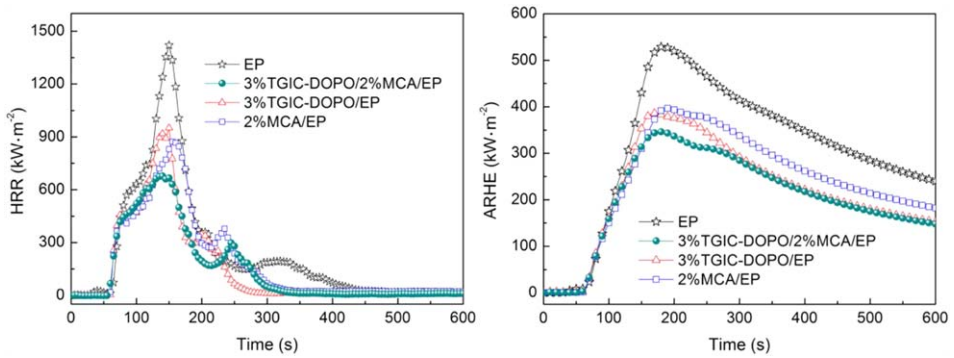

Figure 1. HRR (left) and ARHE (right) curves of the epoxy resin thermosets. [Color figure can be viewed in the online issue, which is available at wileyonlinelibrary.com.]

Table III. Heat and Residue Parameters Collected in the Cone Calorimetry Test

Sample	PHRR (kW/m^2)	av-EHC (MJ/kg)	THR (MJ/m^2)	Maximum ARHE (kW/m^2)	Residue at 600 s (wt %)
EP	1420 ± 53	29.9 ± 0.3	144 ± 5	529 ± 17	7.85 ± 0.22
3% TGIC–DOPO/2% MCA/EP	677 ± 28	19.6 ± 0.2	89 ± 3	346 ± 12	10.75 ± 0.25
3% TGIC–DOPO/EP	951 ± 33	20.0 ± 0.2	91 ± 3	386 ± 13	8.85 ± 0.19
2% MCA/EP	873 ± 30	22.9 ± 0.2	110 ± 3	397 ± 13	4.66 ± 0.13

affords preliminary assessment for judging its further research potential and application values through a clear LOI value and UL94 rating.

To determine the optimal flame-retardant system, TGIC–DOPO/MCA/EP thermosets were prepared and examined. The LOI values and UL94 ratings of the EP thermosets are listed in Table II. With increasing TGIC–DOPO amounts in TGIC–DOPO/MCA/EP, the LOI values also gradually increased. After MCA was incorporated into the TGIC–DOPO/EP thermosets, the LOI values of TGIC–DOPO/MCA/EP were similar to those of TGIC–DOPO/EP containing the same mass fraction of TGIC–DOPO; this revealed that MCA evidently did not affect the LOI value of the TGIC–DOPO/EP thermosets.[40] Usually, MCA just works in the gas phase in flame-retarding polymers, and its flame-retardant effect is relatively weak. Therefore, it was possible that MCA did not increase the LOI value of the thermosets. However, compared with the TGIC–DOPO/EP thermosets, the 3% TGIC–DOPO/2% MCA/EP thermosets passed the UL94 V-0 rating test; this was better than 3% TGIC–DOPO/EP, which achieved a UL94 V-1 rating. This implied that the combination of MCA and TGIC–DOPO resulted in a better flame-retardant effect than the single TGIC–DOPO, although MCA alone contributed little to the flame retardancy of the EP thermoset. The effect of MCA on enhancing the flame retardancy in the vertical burning test was just part of the evidence of its contribution in the TGIC–DOPO/MCA/EP system. In subsequent discussion, more effects of MCA on the flame retardancy are disclosed.

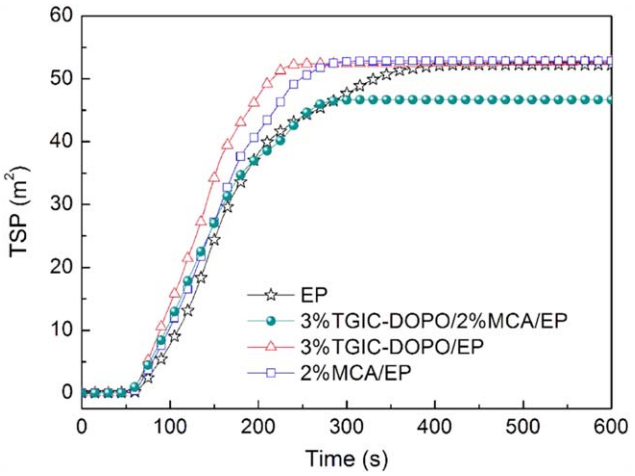

Figure 2. TSP curves of the epoxy resin thermosets. [Color figure can be viewed in the online issue, which is available at wileyonlinelibrary.com.]

In comparison with a previous publication,[40] in this study 3% TGIC–DOPO/2% MCA/EP obtained a similar flame-retardant efficiency as 4% TGIC–DOPO/EP, although MCA barely exerted a flame-retardant effect in the gas phase.[41]

Cone Calorimetry Testing

To further explore the flame-retardant behavior and mechanism of the TGIC–DOPO/MCA composite during combustion, thermosets containing TGIC–DOPO, MCA, and TGIC–DOPO/MCA were individually investigated by cone calorimetry testing. During this testing, MCA caused more outstanding effects in enhancing the flame retardancy of the TGIC–DOPO/MCA/EP thermosets.

Figure 1 shows the curves of the heat-release rate (HRR; left) and average rate of heat emission (ARHE; right), respectively. Compared with that of the neat EP, the peak heat-release rates (PHRRs) evidently decreased in the three flame-retardant EP thermosets. The PHRR of 3% TGIC–DOPO/2% MCA/EP was inhibited to the maximum extent (−52.3%), whereas the PHRRs of 3% TGIC–DOPO/EP and 2% MCA/EP were restrained to a similar level (−33.0 and −38.5%, respectively). Similarly, the maximum ARHE value also presented similar features as the PHRR value. Namely, the maximum ARHE value decreased by 34.6% in 3% TGIC–DOPO/2% MCA/EP, 27.0% in 3% TGIC–DOPO/EP, and 25.0% in 2% MCA/EP. Evidently, TGIC–DOPO and MCA both suppressed the combustion intensity of the EP thermoset to a much lower heat release. However, the two flame retardants had different working mechanisms. TGIC–DOPO mainly exerted a quenching effect through the release of fragments containing phosphorus,[39,40] but MCA mainly exerted a dilution effect by the release of fragments containing nitrogen.[41] The quenching and dilution effects jointly inhibited the combustion intensity and, thus, reduced the HRR

Table IV. CO, CO_2, and Smoke Parameters Collected in the Cone Calorimetry Test

Sample	av-COY (kg/kg)	av-CO_2Y (kg/kg)	TSP (m^2)
EP	0.126 ± 0.005	2.51 ± 0.10	52.2 ± 2.1
3% TGIC–DOPO/2% MCA/EP	0.118 ± 0.004	1.66 ± 0.07	46.6 ± 1.8
3% TGIC–DOPO/EP	0.133 ± 0.005	1.70 ± 0.07	52.8 ± 1.9
2% MCA/EP	0.091 ± 0.004	1.93 ± 0.08	52.8 ± 1.8

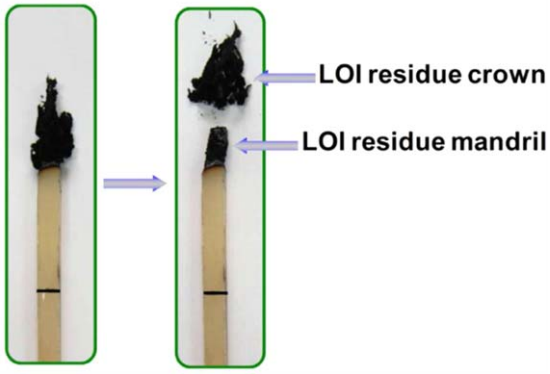

Figure 3. Definition of LOI residue. [Color figure can be viewed in the online issue, which is available at www.interscience.wiley.com.]

values. Moreover, the increased residue yield listed in Table III also reduced the volatile amounts and increased the barrier effect from the char layer. The two factors with flame-inhibition effects jointly inhibited the combustion intensity. Nevertheless, the strongest suppression effect appeared in the test results of 3% TGIC–DOPO/2% MCA/EP. The results demonstrate that the combined application of MCA and TGIC–DOPO imposed better flame retardancy on the thermosets. The results are proposed to have been caused by the interaction between MCA and TGIC–DOPO during combustion; this is backed up by some specific evidence in the following discussion.

In comparison with the previous publication,[40] the PHRR value of 3% TGIC–DOPO/2% MCA/EP was reduced by 34.4% compared with that of 4% TGIC–DOPO/EP. This implied that the incorporation of MCA largely decreased the flame intensity and that the dilution effect of MCA contributed to the flame inhibition effect of the MCA/TGIC–DOPO system.

According to the heat and residue parameters listed in Table III, we also found that 3% TGIC–DOPO/2% MCA/EP was characterized by the lowest average effective heat of combustion (av-EHC) and total heat release (THR). The effective heat of combustion (EHC) is defined as the heat release from the combustion of volatile gas generated from the thermal decomposition of the tested sample, and the EHC value is calculated by the ratio of HRR to the mass loss rate. EHC can be used to measure the combustion status of combustible volatile gas and the intensity of the gaseous-phase flame-retardant effect. Hence, compared with the TGIC–DOPO/EP thermoset, the lowest av-EHC of 3% TGIC–DOPO/2% MCA/EP proved that the addition of MCA effectively inhibited combustion in the gas phase and indeed enhanced the gaseous-phase flame-retardant effect. The results were probably caused by the quenching effect from the fragments containing phosphorus of the pyrolyzed TGIC–DOPO and the dilution effect from the fragments containing nitrogen of the pyrolyzed MCA.[41] The joint actions of the two compositions inhibited the combustion of volatiles from the pyrolyzed thermosets.

Meanwhile, although the single MCA weakened the charring capacity of the EP thermoset according to the decreased residue yield of 2% MCA/EP compared to that of the neat EP, 3% TGIC–DOPO/2% MCA/EP acquired the highest residue yield instead; we deduced that the condensed-phase flame-retardant effect of TGIC–DOPO/MCA/EP was improved by the joint action of MCA and TGIC–DOPO.

In addition, to estimate the smoke-release status of the EP thermoset, we obtained the curves of total smoke production (TSP; Figure 2). The related parameters of carbon monoxide (CO), carbon dioxide (CO_2), and smoke are listed in detail in Table IV.

Evidently, compared with neat EP, unlike the changeless amount of smoke but accelerated smoke-release process in both 3% TGIC–DOPO/EP and 2% MCA/EP, a visibly decreased TSP was observed in the case of 3% TGIC–DOPO/2% MCA/EP. Namely, the smoke-release quantity of 3% TGIC–DOPO/2% MCA/EP was clearly reduced, and the smoke-release rate of the thermoset was also effectively inhibited. The reduction in smoke release was caused by the fact that more compositions were reserved in residue. MCA worked jointly with TGIC–DOPO and promoted the locking of more residue in the condensed phase; this reduced the smoke release. This was more evidence for the joint action of MCA and TGIC–DOPO.

The least sum value of average CO yield (av-COY) and average CO_2 yield (av-CO_2Y) in 3% TGIC–DOPO/2% MCA/EP revealed that the complete and incomplete combustion of combustible volatile gas were both efficiently restrained; this was ascribed to the better gaseous-phase flame-retardant effect. The reason was similar to that given in the discussion on HRR and EHC. The increased residue reduced the release of volatiles, and the flame-quenching effect of TGIC–DOPO and the dilution effect of MCA also caused incomplete combustion. Videlicet, CO, CO_2, and the smoke parameters further confirmed the aforementioned implication that the cooperation between TGIC–DOPO and MCA enhanced the flame-retardant effects in both the gaseous and condensed phases and subsequently gave the EP thermoset better flame retardancy.

Table V. Elemental Compositions of LOI Residue

	LOI-RC (wt %)				LOI-RM (wt %)			
Sample	C_{1s}	N_{1s}	O_{1s}	P_{2p}	C_{1s}	N_{1s}	O_{1s}	P_{2p}
EP	86.9 ± 2.1	2.1 ± 0.1	11.1 ± 0.3	—	85.6 ± 1.9	2.8 ± 0.1	11.6 ± 0.3	—
3% TGIC-DOPO/2% MCA/EP	82.2 ± 1.9	2.9 ± 0.1	13.6 ± 0.4	1.3 ± 0.1	80.5 ± 1.8	3.6 ± 0.1	14.6 ± 0.4	1.2 ± 0.1
3% TGIC-DOPO/EP	81.5 ± 1.8	2.4 ± 0.1	14.9 ± 0.4	1.1 ± 0.1	82.8 ± 1.9	3.5 ± 0.1	12.8 ± 0.3	0.9 ± 0.1
2% MCA/EP	84.5 ± 2.1	2.1 ± 0.1	13.4 ± 0.3	—	83.6 ± 2.0	2.6 ± 0.1	13.7 ± 0.3	—

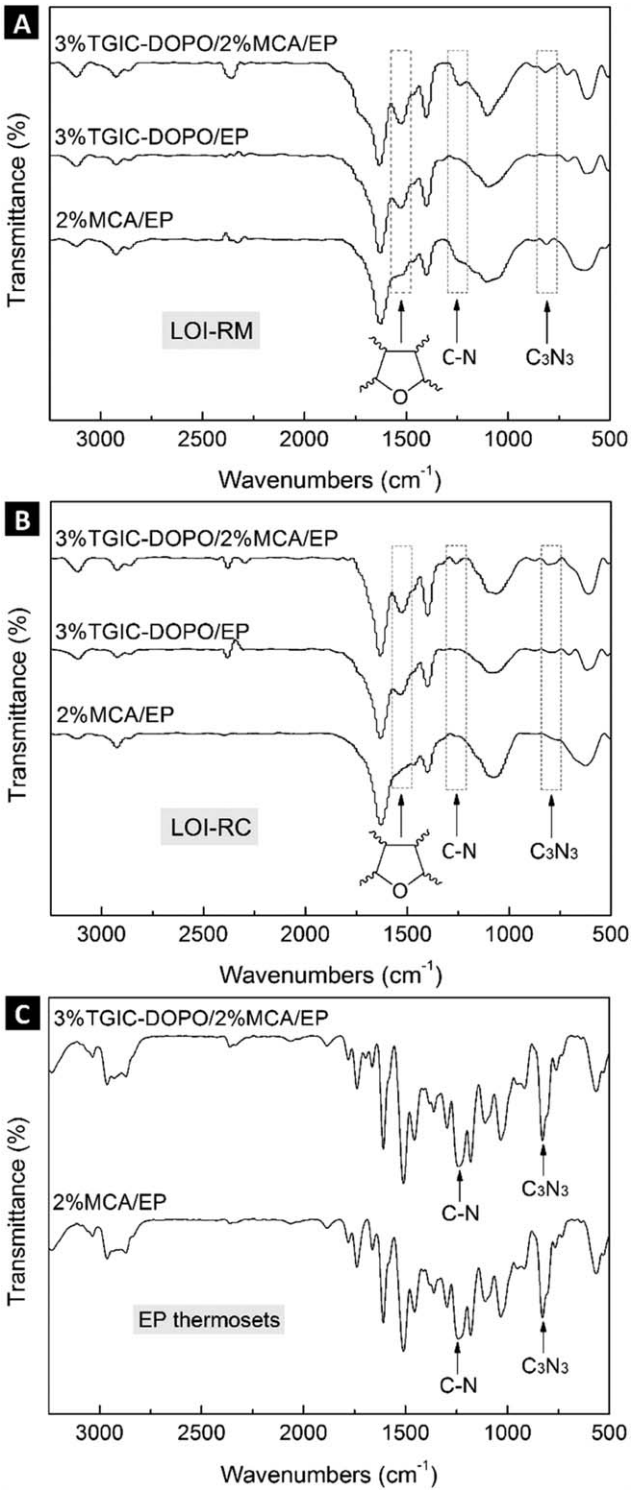

Figure 4. FTIR spectra: (A) LOI-RM, (B) LOI-RC, and (C) flame-retardant EP thermosets.

Elemental Compositions of the LOI Residues

As shown in Figure 3, the LOI residue is divided into two portions: LOI-RC and LOI-RM. LOI-RC consists of light, fluffy, and flocculent residue, whereas LOI-RM consists of rigid and fragile residue.

According to the elemental compositions of LOI-RC and LOI-RM listed in Table V, the existence of the single TGIC–DOPO resulted in more nitrogen and phosphorus being reserved in both parts of the LOI residue compared with the neat EP. On the basis of the conclusions in the former research,[39] we ascribed this to the free-radical quenching effect and promotion effect of the crosslinking and charring from the pyrolytic products of TGIC–DOPO, for example, PO free radicals, isocyanate free radicals, and poly(phosphoric acid) compounds. In 2% MCA/EP, the gaseous-phase flame-retardant effect from the pyrolytic products of MCA just caused a tiny change in the elemental composition of both LOI-RC and LOI-RM. Nevertheless, the combination of TGIC–DOPO and MCA further strengthened the elemental enrichment phenomenon of both nitrogen and phosphorus in 3% TGIC–DOPO/2% MCA/EP. In other words, the coexistence of TGIC–DOPO and MCA made more nitrogen- and phosphorus-containing structures participate in the formation of LOI-RC and LOI-RM. In this process, the increased nitrogen-containing residue could have come from the three nitrogen-containing parts: (1) the EP thermoset, (2) TGIC–DOPO, and (3) MCA. Meanwhile, the increase in the phosphorus-containing residue implied that more phosphorus-containing compound was reserved in the condensed phase; this promoted the charring process of the thermosets. These results were caused by the incorporation of MCA into the TGIC–DOPO/EP system. Therefore, this could have also been indirect evidence of the interaction between TGIC–DOPO and MCA.

FTIR Spectra of the LOI Residue

To further demonstrate the chemical structure of the LOI residue, Figure 4 shows the FTIR spectra of LOI-RC and LOI-RM from 3% TGIC–DOPO/2% MCA/EP, 3% TGIC–DOPO/EP, and 2% MCA/EP.

The FTIR spectra of the different residues showed similar bands because the residues had the same main contents of EP thermoset. However, there were still some tiny differences in these bands; these differences were caused by the different flame retardants incorporated into the EP thermosets. These tiny differences in the bands just revealed the diverse flame-retardant action mode of the additives during combustion. In the spectra

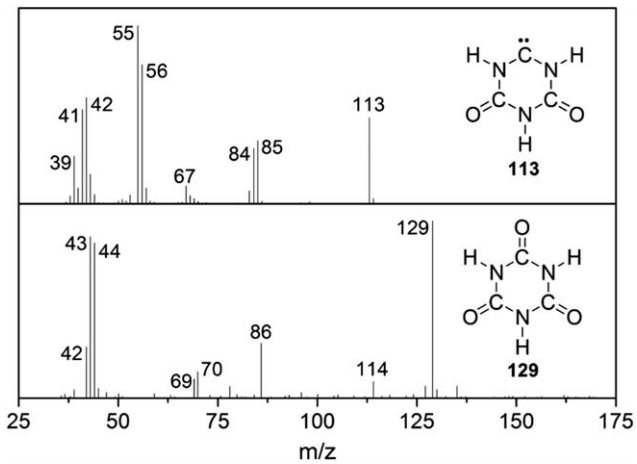

Figure 5. Mass spectrometry spectra of MCA.

of both LOI-RC and LOI-RM, the main differences appeared in the bands near 807, 1260, and 1526 cm^{-1}. The band at 807 cm^{-1} corresponded to the bending vibrations of the triazine ring (C_3N_3), and the band at 1260 cm^{-1} corresponded to the C—N vibrations.[42–44] As the mass spectrometry spectra shows in Figure 5, the mass-to-charge ratio (m/z) values of 113 and 129 corresponded to the two triazine fragments, respectively. This revealed that MCA mainly decomposed to triazine fragments after combustion. Because of the incorporation of MCA, the FTIR spectra of the 3% TGIC–DOPO/2% MCA/EP residue showed the extra 807 and 1260 cm^{-1} vibrations. According to the previous discussion, the two vibrations should have resulted from the C_3N_3 and C—N structures in the triazine fragments. In addition, both bands appeared in LOI-RM of 2% MCA/EP and did not emerge in that of 3% TGIC–DOPO/EP, as shown in Figure 4(A). This revealed that some triazine fragments of MCA were reserved in residue. Meanwhile, the two bands also appeared in LOI-RM of 3% TGIC–DOPO/2% MCA/EP more clearly; this implied that more triazine fragments of MCA were reserved when MCA and TGIC–DOPO were applied jointly in the EP thermoset. This deduction was further supported by the spectra of LOI-RC. As shown in Figure 4(B), the bands near 807 and 1260 cm^{-1} were not clearly observed in the spectrum of either 2% MCA/EP or 3% TGIC–DOPO/EP, but they appeared in the spectrum of 3% TGIC–DOPO/2% MCA/EP. These results show that the triazine fragments of MCA in the gaseous phase combined with larger fragments of the matrix[40] and were finally reserved in LOI-RM, whereas MCA and TGIC–DOPO were applied together in the EP thermoset. This not only confirmed the interaction between MCA and TGIC–DOPO but also provided definite interaction evidence to support the previous inference that the cooperation between MCA and TGIC–DOPO obtained a more efficient flame-retardant effect than that of the single TGIC–DOPO.

In addition, the band at 1526 cm^{-1} only appeared in the residues of 3% TGIC–DOPO/EP and 3% TGIC–DOPO/2% MCA/EP; it should have been formed by TGIC–DOPO pyrolysis. According to the former research,[39] this band was ascribed to the dibenzofuran derivatives from the decomposed phosphaphenanthrene group in TGIC–DOPO. Because the residue of 3% TGIC–DOPO/2% MCA/EP simultaneously possessed the flame-retardant traces of TGIC–DOPO and MCA, this implied that the excellent flame retardancy of 3% TGIC–DOPO/2% MCA/EP came from the joint action of TGIC–DOPO and MCA.

CONCLUSIONS

The triazine-rich compound MCA and bigroup compound TGIC–DOPO were jointly incorporated into EP thermosets to explore more efficient flame-retardant systems. The 3% TGIC–DOPO/2% MCA/EP thermoset showed a lower PHRR, EHC value, amount of total smoke products, and total yield of CO and CO_2 than the 3% TGIC–DOPO/EP. The results reveal that MCA and TGIC–DOPO worked jointly in the flame-retardant thermosets. The dilution effect of MCA, the quenching effect of TGIC–DOPO, and their joint action inhibited the combustion intensity and imposed better flame-retardant effects in the gas phase. The 3% TGIC–DOPO/2% MCA/EP thermosets also exhibited an increased residue yield, and more compositions with triazine rings were locked in the residues; this implied that MCA/TGIC–DOPO worked jointly in the condensed phase and promoted thermoset charring. The results reveal the better flame-retardant effect of the MCA/TGIC–DOPO system in condensed phase. In summary, the joint incorporation of MCA and TGIC–DOPO into the EP thermosets increased the flame-retardant effects in both the condensed and gas phases during combustion.

ACKNOWLEDGMENTS

Financial support was provided by the National Nature Science Funds (contract grant number 21374003) and the Plans to Upgrade Beijing Municipal Innovation Ability (contract grant number TJSHG201510011021).

REFERENCES

1. Dasari, A.; Yu, Z. Z.; Cai, G. P.; Mai, Y. W. *Prog. Polym. Sci.* **2013**, *38*, 1357.
2. Sorathia, U.; Ness, J.; Blum, M. *Compos. A* **1999**, *30*, 707.
3. Mngomezulu, M. E.; John, M. J.; Jacobs, V.; Luyt, A. S. *Carbohydr. Polym.* **2014**, *111*, 149.
4. Tirri, T.; Aubert, M.; Pawelec, W.; Wilén, C. E.; Pfaendner, R.; Hoppe, H.; Roth, M.; Sinkkonen, J. *J. Appl. Polym. Sci.* **2014**, *131*, 40413.
5. El Gouri, M.; El Bachiri, A.; Hegazi, S. E.; Rafik, M.; El Harfi, A. *Polym. Degrad. Stab.* **2009**, *94*, 2101.
6. Wang, C. S.; Lin, C. H. *J. Polym. Sci. Part A: Polym. Chem.* **1999**, *37*, 3903.
7. Franchini, E.; Galy, J.; Gérard, J. F.; Tabuani, D.; Medici, A. *Polym. Degrad. Stab.* **2009**, *94*, 1728.
8. Seefeldt, H.; Duemichen, E.; Braun, U. *Polym. Int.* **2013**, *62*, 1608.
9. Mathew, D.; Nair, C. P. R.; Ninan, K. N. *Polym. Int.* **2000**, *49*, 48.
10. Xuan, S. Y.; Wang, X.; Song, L.; Xing, W. Y.; Lu, H. D.; Hu, Y. *Polym. Int.* **2011**, *60*, 1541.
11. Liu, S. M.; Chen, J. B.; Zhao, J. Q.; Jiang, Z. J.; Yuan, Y. C. *Polym. Int.* **2015**, *64*, 1182.
12. Laoutid, F.; Bonnaud, L.; Alexandre, M.; Lopez-Cuesta, J. M.; Dubois, P. *Mater. Sci. Eng. Rep.* **2009**, *63*, 100.
13. Wang, X.; Song, L.; Yang, H. Y.; Xing, W. Y.; Kandola, B.; Hu, Y. *J. Mater. Chem.* **2012**, *22*, 22037.
14. Wang, L. C.; Jiang, J. Q.; Jiang, P. K.; Yu, J. H. *J. Polym. Res.* **2010**, *17*, 891.
15. Song, P. A.; Liu, H.; Shen, Y.; Du, B. X.; Fang, Z. P.; Wu, Y. *J. Mater. Chem.* **2009**, *19*, 1305.
16. Yang, W.; Song, L.; Hu, Y.; Lu, H. D.; Yuen, R. K. K. *Compos. B* **2011**, *42*, 1057.
17. Braun, U.; Schartel, B. *Macromol. Mater. Eng.* **2008**, *293*, 206.
18. Tang, L. S.; Yuan, Z. G.; Xu, L.; Li, X.; Ge, Y. Z. *Adv. Mater. Sci. Eng.* **2013**, *2013*, 1.

19. Friederich, B.; Laachachi, A.; Ferriol, M.; Cochez, M.; Sonnier, R.; Toniazzo, V.; Ruch, D. *Polym. Degrad. Stab.* **2012**, *97*, 2154.
20. Su, X. Q.; Yi, Y. W.; Tao, J.; Qi, H. Q.; Li, D. Y. *Polym. Degrad. Stab.* **2014**, *105*, 12.
21. Xu, M. L.; Chen, Y. J.; Qian, L. J.; Wang, J. Y.; Tang, S. *J. Appl. Polym. Sci.* **2014**, *131*, 41006.
22. Lai, X. J.; Zeng, X. R.; Li, H. Q.; Liao, F.; Yin, C. Y.; Zhang, H. L. *Polym. Compos.* **2012**, *33*, 35.
23. Li, J.; Ke, C. H.; Xu, L.; Wang, Y. Z. *Polym. Degrad. Stab.* **2012**, *97*, 1107.
24. Rakotomalala, M.; Wagner, S.; Döring, M. *Materials* **2010**, *3*, 4300.
25. Mohan, P. *Polym.-Plast. Technol.* **2013**, *52*, 107.
26. Mercado, L. A.; Ribera, G.; Galià, M.; Cádiz, V. *J. Polym. Sci. Part A: Polym. Chem.* **2006**, *44*, 1676.
27. Ananda Kumar, S.; Denchev, Z.; Alagar, M. *Eur. Polym. J.* **2006**, *42*, 2419.
28. Qian, L. J.; Ye, L. J.; Xu, G. Z.; Liu, J.; Guo, J. Q. *Polym. Degrad. Stab.* **2011**, *96*, 1118.
29. Qian, L. J.; Ye, L. J.; Qiu, Y.; Qu, S. R. *Polymer* **2011**, *52*, 5486.
30. Qian, L. J.; Qiu, Y.; Liu, J.; Xin, F.; Chen, Y. J. *J. Appl. Polym. Sci.* **2014**, *131*, 39709.
31. Perez, R. M.; Sandler, J. K. W.; Altstädt, V.; Hoffmann, T.; Pospiech, D.; Ciesielski, M.; Döring, M. *J. Mater. Sci.* **2006**, *41*, 341.
32. Schartel, B.; Balabanovich, A. I.; Braun, U.; Knoll, U.; Artner, J.; Ciesielski, M.; Döring, M.; Perez, R.; Sandler, J. K. W.; Altstädt, V.; Hoffmann, T.; Pospiech, D. *J. Appl. Polym. Sci.* **2007**, *104*, 2260.
33. Perret, B.; Schartel, B.; Stöß, K.; Ciesielski, M.; Diederichs, J.; Döring, M.; Krämer, J.; Altstädt, V. *Eur. Polym. J.* **2011**, *47*, 1081.
34. Perret, B.; Schartel, B.; Stöß, K.; Ciesielski, M.; Diederichs, J.; Döring, M.; Krämer, J.; Altstädt, V. *Macromol. Mater. Eng.* **2011**, *296*, 14.
35. Müllera, P.; Bykovb, Y.; Döring, M. *Polym. Adv. Technol.* **2013**, *24*, 834.
36. Patrick Lim, W. K.; Mariatti, M.; Chow, W. S.; Mar, K. T. *Compos. B* **2012**, *43*, 124.
37. Zhang, K.; Wu, K.; Zhang, Y. K.; Liu, H. F.; Shen, M. M.; Hu, W. G. *Polym.-Plast. Technol.* **2013**, *52*, 525.
38. Zhang, W. C.; Li, X. M.; Yang, R. *J. Polym. Degrad. Stab.* **2014**, *99*, 118.
39. Qian, L. J.; Qiu, Y.; Sun, N.; Xu, M. L.; Xu, G. Z.; Xin, F.; Chen, Y. *J. Polym. Degrad. Stab.* **2014**, *107*, 98.
40. Qian, L. J.; Qiu, Y.; Wang, J. Y.; Xi, W. *Polymer* **2015**, *68*, 262.
41. Tang, S.; Qian, L. J.; Qiu, Y.; Sun, N. *J. Appl. Polym. Sci.* **2014**, *131*, 40558.
42. Dante, R. C.; Martín-Ramos, P.; Sánchez-Arévalo, F. M.; Huerta, L.; Bizarro, M.; Navas-Gracia, Luis, M.; Martín-Gil, J. *J. Solid State Chem.* **2013**, *201*, 153.
43. Dante, R. C.; Martín-Ramos, P.; Correa-Guimaraes, A.; Martín-Gil, J. *Mater. Chem. Phys.* **2011**, *130*, 1094.
44. Foy, D.; Demazeau, G.; Florian, P.; Massiot, D.; Labrugère, C.; Goglio, G. *J. Solid State Chem.* **2009**, *182*, 165.